Universitat Polytechnica de Catalunya
MSc Computational Mechanics
Spring 2018

Finite Elements in Fluids

FEFmatlab3

Due 02/04/2018

Alexander Keiser

1 Inclusion of GLS Method and Triangular Quadratic Elements

We will first begin by including the Galerkin Least Squares method within the provided codes, this will be done in the FEMsystem.m code file and can be seen in figure 1 below with code and associated comments.

```
    elseif method == 3 %GALERKIN LEAST SQUARES METHOD

        %Here we have a variable aux made from nodal coordinates
        %multiplied with shape functions
        aux = N_ig*Xe;

        %Here we are defining the reaction term using RT notation
        %calling from another created function file
        RT_ig = RT(aux);

        %Here we generate the stiffness matrix K
        Ke = Ke + (nu*(Nx'*Nx+Ny'*Ny) + N_ig'*(ax*Nx+ay*Ny)+...
            N_ig'*RT_ig*N_ig + tau*((((ax*Nx+ay*Ny)-nu*(Nxx+Nyy)+ ...
            RT_ig*N_ig)'*((ax*Nx+ay*Ny)-nu*(Nxx+Nyy)+RT_ig*N_ig)))...
            *dvolu;

        %Here we are defining the source term using ST notation
        %calling from another created function file
        f_ig = ST(aux);

        %Here we have generation of force vector
        fe = fe + (N_ig+tau*((ax*Nx+ay*Ny)-nu*(Nxx+Nyy)))'*(f_ig*dvolu);

    else
```

Figure 1: Inclusion of GLS method into System.m file

Now that we have included the GLS method, we will include the Triangular Quadratic element code. This will be done in the ShapeFunc.m file and can be seen in figure 2 on the next page.

```
%IMPLEMENTATION OF THE TRIANGULAR QUADRATIC ELEMENT
elseif p == 2
    N = [ xi.*(2*xi-1), eta.*(2*eta-1), (1-xi-eta).*(2*(1-xi-eta)-1),...
        4*xi.*eta, 4*eta.*(1-xi-eta), 4*(1-xi-eta).*xi];

    Nxi = [ 4*xi - 1, zeros(size(xi)), 4*eta + 4*xi - 3,...
        4*eta, -4*eta, 4 - 8*xi - 4*eta];

    Neta = [ zeros(size(xi)), 4*eta - 1, 4*eta + 4*xi - 3,...
        4*xi, 4 - 4*xi - 8*eta, -4*xi];

    N2xi = [ 4*ones(size(xi)), 0*ones(size(xi)), 4*ones(size(xi)),...
        0*ones(size(xi)), 0*ones(size(xi)), -8*ones(size(xi))];

    N2eta = [  0*ones(size(xi)), 4*ones(size(xi)), 4*ones(size(xi)),...
        0*ones(size(xi)), -8*ones(size(xi)), 0*ones(size(xi))];



else
```

Figure 2: Inclusion of the triangular quadratic element code in the ShapeFunc.m file

Now that w have included the necessary codes, we will verify that the method is functional for all 4 types of element. This can be seen in the following figures.

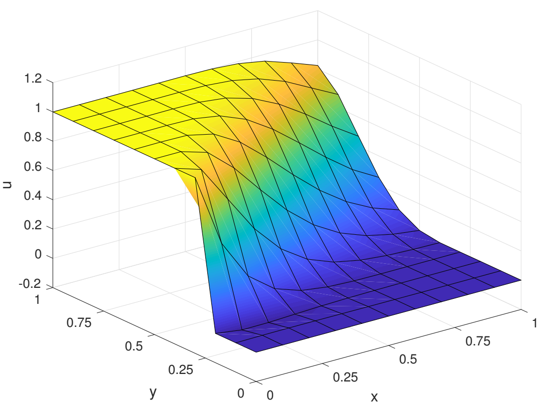

Figure 3a: GLS 10 linear quadrilateral elements (LQE)

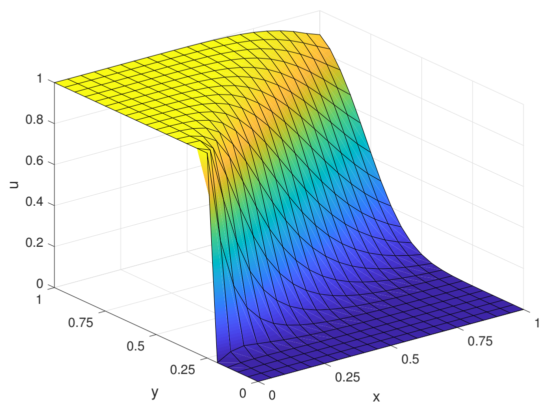

Figure 3b: GLS 10 quadratic quadrilateral elements (QQE)

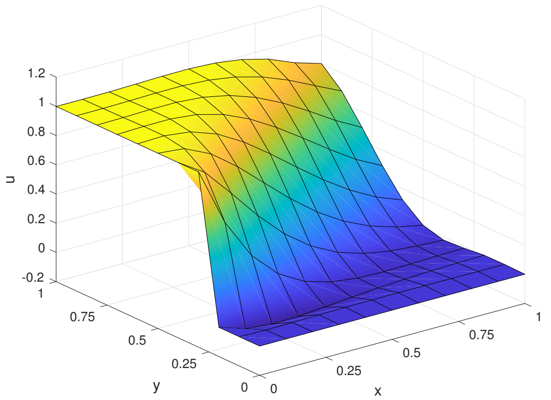

Figure 3c: GLS 10 linear triangular elements (LTE)

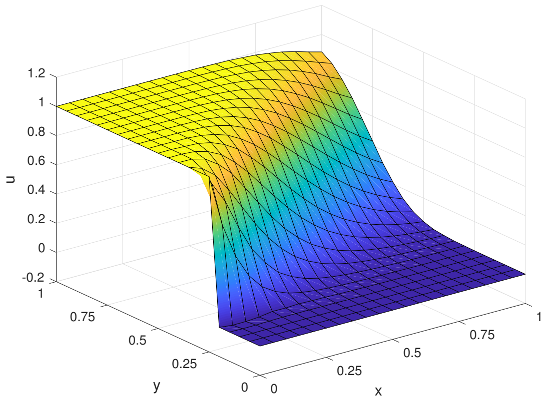

Figure 3d: GLS 10 quadratic triangular elements (QTE)

Here we can see the results of the Galerkin Least Squares approximation method for bot linear/quadratic triangular/quadrilateral elements. From the Figures we can see that there is no significant difference between the linear implementations of each element type. The same can also be said about the quadratic implementation of each element type. However, it can be said that both quadratic elements types are much more accurate than that their linear counterparts.

2 Imposition of Zero Dirichlet Boundary Conditions

We will now modify the codes to solve a steady convection-diffusion reaction problem with zero Dirichlet boundary conditions on the outlet boundary. We will then compare the new GLS method's behavior to the previously observed Neumann imposed boundary conditions. We will then solve the codes for some specified values. The modified GLS method behavior can be seen in the figures below.

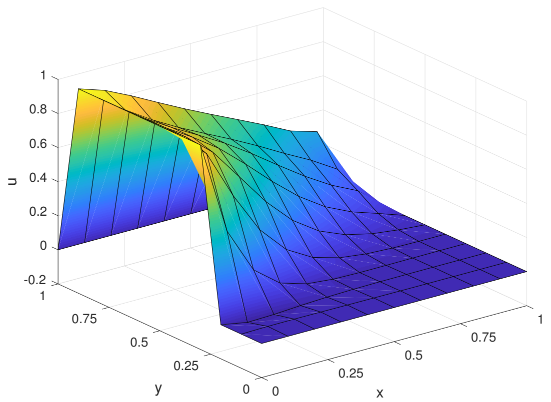

Figure 4a: Modified GLS 10 LQE

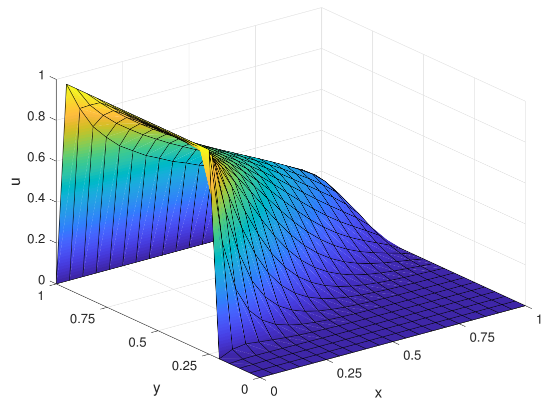

Figure 4b: Modified GLS 10 QQE

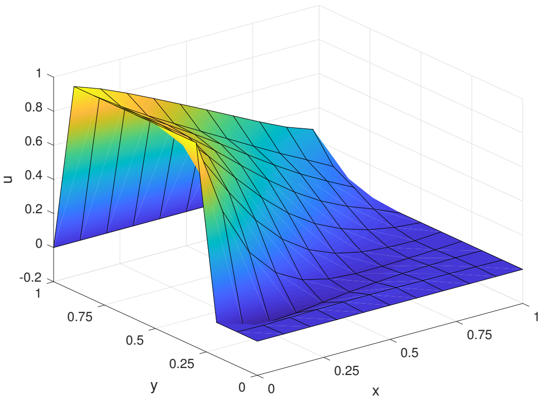

Figure 4c: Modified GLS 10 LTE

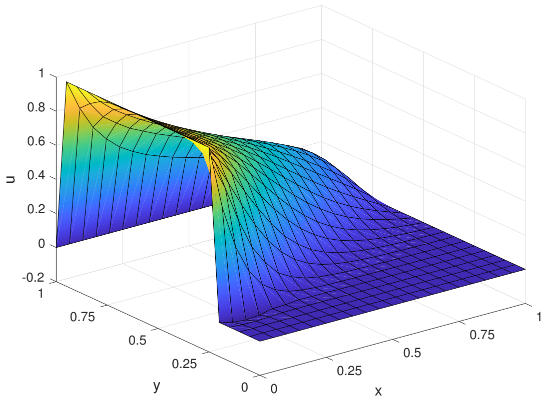

Figure 4d: Modified GLS 10 QTE

Above we have successfully imposed the prescribed zero dirichlet boundary condition for all of the previous cases. The first and most blatant observation that can be made is the apparent spike that is present in both linear cases but not present in the quadratic cases. This spike is due primarily to the oscillatory behavior exhibited by the Galerkin Least Squares approximation method when trying to enforce a prescribed dirichlet condition. It is no where near as definitive in the quadratic case counterparts because of the increased number of degrees of freedom captured by these element types. We will now draw some additional comparisons between the 2 sets of figures, this can be seen below.

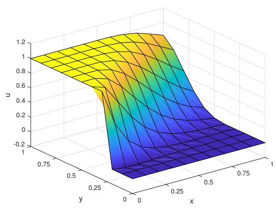

GLS 10 LQE

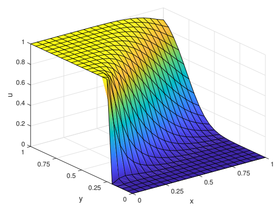

GLS 10 QQE

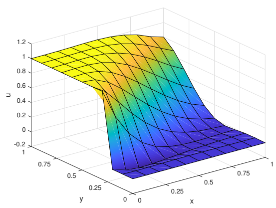

GLS 10 LTE

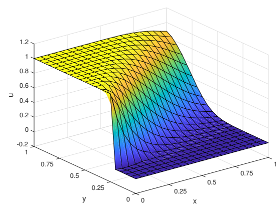

GLS 10 QTE

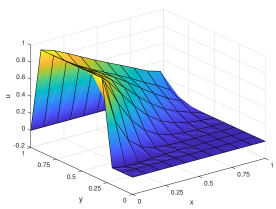

M GLS 10 LQE

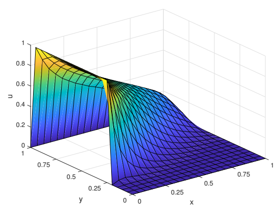

M GLS 10 QQE

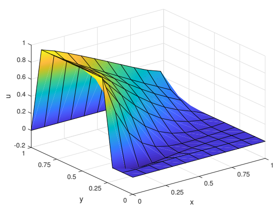

M GLS 10 LTE

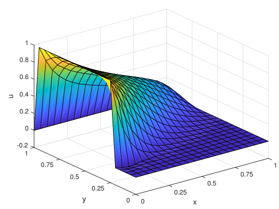

M GLS 10 QTE

Here we have all four original solutions above their modified counterparts. It is apparent from these graphs that the quadratic element types give a significant increase in accuracy in the solution, this is to be expected and is consistant with the theory. It worth noting that these Galerkin Least Squares approximations exhibit a bigger dip along the central-diagonal wave front, this is also due primarily to the oscillatory behavior exhibited by the Galerkin Least Squares approximation method, and coincides with the theory nicely.

We will now solve the specified problems using Galerkin Least Squares approximation with quadratic quadrilateral elements. We will use quadrilateral elements because they better fit our square geometry and will use quadratic elements because the produce results of higher accuracy as has been shown previously in this report.

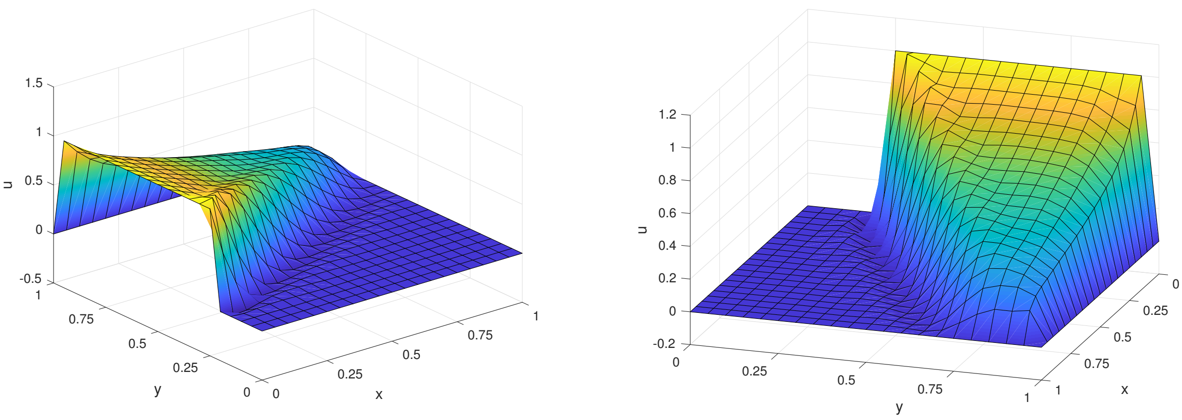

Figure 5: Two views of GLS solution to convection-reaction dominated case

Here we have 2 views of the same solution to a convection-reaction dominated case of the 2D steady transport problem. The problem parameters are as follows, the convection coefficient a=0.5, the diffusion coefficient $\nu = 0.0001$, and the reaction term $\sigma = 1$. On the right hand figure above we can notice a semi-abrupt transition to the imposed dirichlet boundary condition when compared to the reaction dominated case on the following page. This is a result of the extremely low value of the diffusion coefficient not allowing as much velocity to diffuse from the system as in the reaction dominated case on the next page.

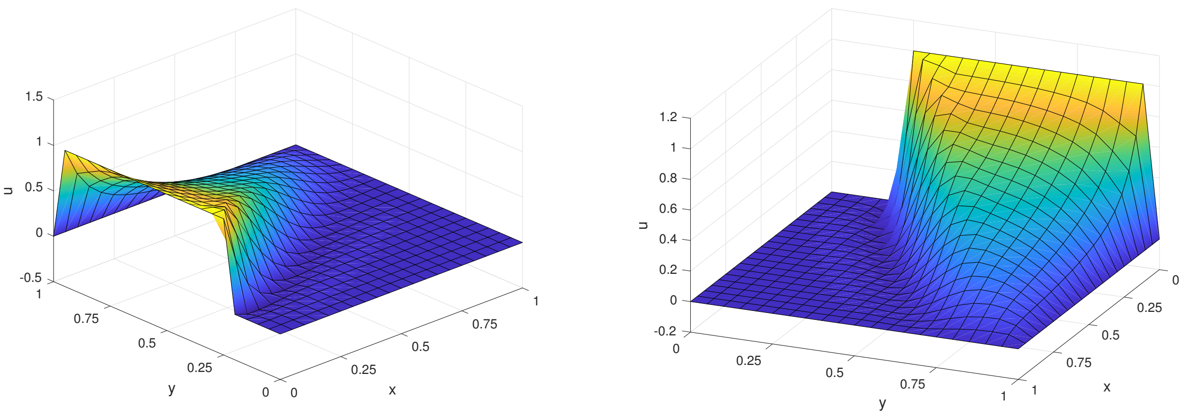

Figure 6: Two views of GLS solution to reaction dominated case

Similarly to what we have seen in figure 5, above in figure 6 we can see two views of the same solution to a reaction dominated case of this problem. The problem parameters are as follows, the convection coefficient a=0.001, the diffusion coefficient $\nu = 0.0001$, and the reaction term $\sigma = 1$. We can notice that the once semi-abrupt transition described above is now much smoother and gradual. This is a result of the decreased relative convection value allowing more velocity to diffuse out of the prescribed dirichlet boundary than in the convection-reaction case presented above in figure 5.